AJNR

Quantitative Evaluation and Visualization of Lumbar Foraminal Nerve Root Entrapment by Using Diffusion Tensor Imaging: Preliminary Results

Y. Eguchi, S. Ohtori, S. Orita, H. Kamoda, G. Arai, T. Ishikawa, M. Miyagi, G. Inoue, M. Suzuki, Y. Masuda, H. Andou, M. Takaso, Y. Aoki, T. Toyone, A. Watanabe and K. Takahashi

AJNR Am J Neuroradiol 2011, 32 (10) 1824-1829
doi: https://doi.org/10.3174/ajnr.A2681
http://www.ajnr.org/content/32/10/1824

ORIGINAL RESEARCH

Quantitative Evaluation and Visualization of Lumbar Foraminal Nerve Root Entrapment by Using Diffusion Tensor Imaging: Preliminary Results

Y. Eguchi
S. Ohtori
S. Orita
H. Kamoda
G. Arai
T. Ishikawa
M. Miyagi
G. Inoue
M. Suzuki
Y. Masuda
H. Andou
M. Takaso
Y. Aoki
T. Toyone
A. Watanabe
K. Takahashi

BACKGROUND AND PURPOSE: DTI can provide valuable structural information that may become an innovative tool in evaluating lumbar foraminal nerve root entrapment. The purpose of this study was to visualize the lumbar nerve roots and to measure their FA in healthy volunteers and patients with lumbar foraminal stenosis by using DTI and tractography with 3T MR imaging.

MATERIALS AND METHODS: Eight patients with lumbar foraminal stenosis and 8 healthy volunteers underwent 3T MR imaging. In all subjects, DTI was performed with echo-planar imaging at a b-value of 800 s/mm^2 and the lumbar nerve roots were visualized with tractography. Mean FA values in the lumbar nerve roots were quantified on DTI images.

RESULTS: In all subjects, the lumbar nerve roots were clearly visualized with tractography. In all patients, tractography also showed abnormalities such as tract disruption, nerve narrowing, and indentation in their course through the foramen. Mean FA values were significantly lower in entrapped roots than in intact roots.

CONCLUSIONS: We demonstrated that DTI and tractography of human lumbar nerves can visualize and quantitatively evaluate lumbar nerve entrapment with foraminal stenosis. We believe that DWI is a potential tool for the diagnosis of lumbar nerve entrapment.

ABBREVIATIONS: FA = fractional anisotropy; MPG = motion probing gradient; VAS = visual analog scale

In patients with degenerative lumbar disease, lumbar foraminal stenosis often causes nerve root entrapment, which is characterized by radicular symptoms affecting the leg.[1-6] This condition may unfortunately result in failed back surgery syndrome because of the difficulty in making a correct diagnosis and is a cause of continued postoperative pain.[7,8] Conventional MR imaging has been inadequate for evaluating symptomatic foraminal stenosis, because of the high incidence of false-positives found in asymptomatic elderly patients.[9] New diagnostic imaging techniques to detect lumbar nerve root entrapment are urgently required.

DWI based on MR imaging can provide valuable information regarding the microstructure of tissues by applying an MPG in some directions to monitor the random movement of water molecules, which is restricted in tissues.[10-13] DWI has been widely used clinically in the evaluation of the central nervous system for the diagnosis of diseases such as acute brain stroke.[14] If there is no directional variation rate in tissues, diffusion is said to be isotropic. In contrast, in neural tissue water molecules tend to move along the nerve fibers, and this is called anisotropic diffusion. Nerve tractography uses DTI to visualize highly anisotropic nerve fiber tracts. The diffusion data can be used for the determination of quantitative diffusion values such as the ADC and a scalar FA value that reflects the directionality of molecular diffusion. FA values range from 0 to 1, with high FA values indicating anisotropic diffusion and low FA values indicating more isotropic diffusion.

Recently, several studies have shown that DTI is useful for the evaluation and visualization of peripheral nerves[15] and the measurement of axon regeneration in rat[16] and mouse[17] sciatic nerves, demonstrating that a decrease in mean FA values was observed in injured nerves with demyelination.[15-18]

Imaging of the spinal cord is challenging because of technical limitations such as the relatively small size of the cord, susceptibility artifacts because of tissue-bone interfaces, and the motion artifacts arising from respiratory activity.[19]

Although we reported previously that DWI of lumbar nerves by using 1.5T MR imaging could visualize and quantitatively evaluate lumbar nerve entrapment with foraminal stenosis,[20] to date, quantitative DTI has not been applied to evaluate the pathology of lumbar nerve root entrapment. Nerve root entrapment may contribute to radicular symptoms in

Received December 31, 2010; accepted after revision March 9, 2011.

From the Department of Orthopaedic Surgery (Y.E., S.Oh., S.Or., H.K., G.A., T.I., M.M., G.I., M.S., K.T.), Graduate School of Medicine, Chiba University, Chuo-ku, Chiba, Japan; Department of Radiology (Y.M., H.A.), Chiba University Hospital, Chuo-ku, Chiba, Japan; Department of Orthopaedic Surgery (M.T.), School of Medicine, Kitasato University, Sagamihara City, Kanagawa, Japan; Department of Orthopedic Surgery (Y.A.), Chiba Rosai Hospital, Ichihara, Chiba, Japan; and Department of Orthopaedic Surgery (T.T., A.W.), Teikyo University Chiba Medical Center, Chiba, Japan.

All subjects were studied after informed consent, and the study had prior approval of the Chiba University Ethics Committee.

Please address correspondence to Yawara Eguchi, MD, PhD, Department of Orthopaedic Surgery, Graduate School of Medicine, Chiba University, 1-8-1 Inohana, Chuo-ku, Chiba, 260-8670, Japan; e-mail address: yawara_eguchi@yahoo.co.jp

http://dx.doi.org/10.3174/ajnr.A2681

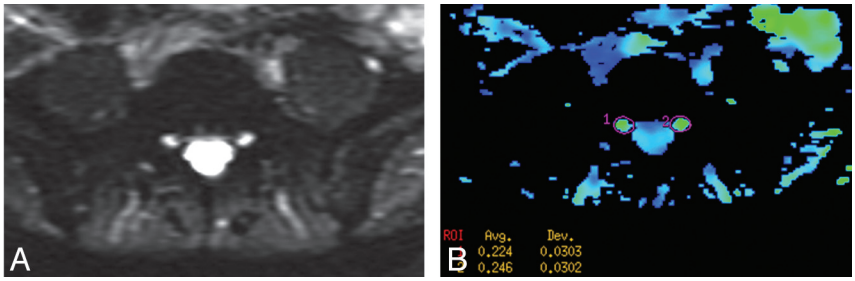

Fig 1. Echo-planar imaging image (*A*) and FA mapping (*B*) ROIs were placed on bilateral roots and FA values were calculated (*B*)

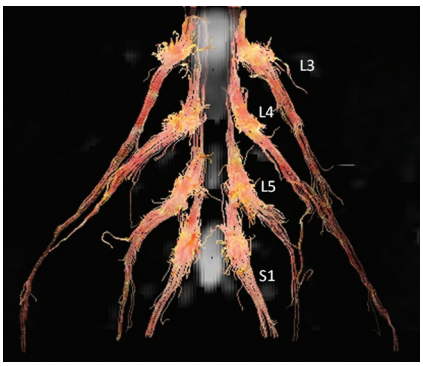

Fig 2. Coronal tractogram of lumbar nerve roots in a healthy volunteer. L3, L4, L5, and S1 indicate the third, fourth, and fifth lumbar root, and the first sacral root.

patients with lumbar foraminal stenosis. The purpose of this study was to measure the FA of lumbar and sacral nerve roots in healthy volunteers and in patients with lumbar foraminal stenosis by using MR imaging at 3T. This study also investigated whether tractography is useful for visualizing lumbar foraminal nerve root entrapment.

Materials and Methods

Subjects

Eight patients (5 men, 3 women; median age, 61.0 years, range, 44–75 years) who had unilateral radicular symptoms affecting leg pain with lumbar foraminal stenosis and without central lumbar canal stenosis were studied by using MR imaging. Eight healthy volunteers (5 men, 3 women; median age, 46 years; range, 37–55 years) served as controls. Their diagnoses were based on neurologic symptoms; a selective nerve root block; and a combination of diagnostic images, including plain radiographs, CT, and MR imaging. This study included those patients in whom performing a selective nerve root block accurately diagnosed the location of symptomatic nerve roots. The location of symptomatic foraminal stenosis in all 8 patients was L5 nerve roots. A total of 64 L4 and L5 foramens and corresponding nerve roots (4 foramens/person) in 8 patients and 8 volunteer controls also were analyzed with MR imaging and DTI to investigate diagnostic performance. The patient exclusion criteria were as follows: 1) those who had lumbar spine surgery before this DWI study, 2) those who had multiple levels of lumbar canal stenosis, and 3) those who had myelopathy. The mean duration of sciatic pain before MR imaging was 16.2 months (range, 7–24 months). The leg pain was evaluated by using a VAS scoring system from 100 (extreme amount of pain) to 0 (no pain). In this study, all of the patients underwent conservative treatment.

Table 1: Mean FA values of healthy volunteers

	FA (Proximal)		FA (Distal)	
Root	Right	Left	Right	Left
L3	0.157 ± 0.028	0.161 ± 0.032	0.172 ± 0.022	0.196 ± 0.047
L4	0.183 ± 0.017	0.190 ± 0.027	0.188 ± 0.031	0.185 ± 0.029
L5	0.196 ± 0.020	0.192 ± 0.020	0.220 ± 0.030	0.214 ± 0.037
S1	0.195 ± 0.030	0.192 ± 0.040	0.212 ± 0.032	0.205 ± 0.040

MR Imaging Protocol

A 1.5T MR imaging scanner (Philips Medical Systems, Best, the Netherlands) was used in this study. Sagittal T1-weighted (TR/TE, 400/14), axial, and sagittal T2-weighted fast spin-echo (TR/TE, 4000/102) sequences were obtained by using a 256 × 256 matrix, 260-mm FOV, and 3/1-mm section thickness/gap.

DTI Protocol

A 3T MR imaging scanner (Discovery MR750; GE Healthcare, Milwaukee, Wisconsin) was used in this study. Subjects were scanned in a supine position by using a Sense XL Torso coil. DTI was performed by using array special sensitivity encoding technique, factor: 2; chemical shift selective suppression; and an echo-planar imaging sequence with a free-breathing scanning technique. The following imaging parameters were set: 800 s/mm^2 b-value; MPG, 11 directions; 6000/76 ms for TR/TE, respectively; axial section orientation, 3/0-mm section thickness/gap; 320 × 256 mm FOV; 96 × 192 matrix; 3.3 × 1.66 × 3.0-mm^3 actual voxel size; 1.6 × 1.6 × 4.0-mm^3 calculated voxel size; 4 excitations; 50 total sections; and 4 minutes 54 seconds scan time.

Image Analysis

After DTI data were transferred to a PC, Volume-One (http://www.volume-one.org/) and dTVIISR (diffusion TENSOR Visualizer II) software (second release; http://www.ut-radiology.umin.jp/people/masutani/dTV.htm)[21] were used for tractography and FA mapping (Fig 1). The diffusion tensor was calculated by using a log-linear fitting method. The ROIs were placed at 2 levels of the nerve root: proximal and distal to the lumbar foraminal zone. FA was calculated with the software at the 2 levels of the nerve root from L3 to S1 in patients and healthy volunteers. The size of ROIs from 25 to 50 mm^2 was selected to be as accurate as possible on the respective nerve roots to avoid partial volume effects when the mean FA was calculated. In this study, CSF contamination effects were considered to be negligible because section thickness was 3 mm and therefore smaller than the L5 dorsal root ganglia size, which was 5 mm wide and 10 mm long. All DTI analyses were performed twice by 2 trained spine surgeons to evaluate intra- and interobserver differences. The evaluation of tractography included abnormalities of nerve root such as disruption, narrowing, and indentation.

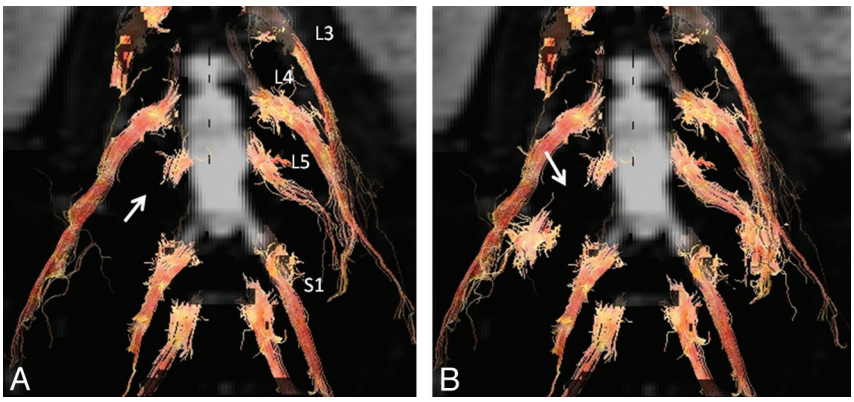

Fig 3. Tractograms of lumbar nerve roots in a 75-year-old man with right L5–S1 foraminal stenosis (referenced as patient 1 in Table 3) by ROI placement on bilateral L5 roots at the stenotic level. ROIs were placed both proximally and distally to the foraminal zone at the nonstenotic level of L3, L4, and S1 roots. On the entrapped side of the right L5 root, by placing the region of interest on the proximal side (*A*), nerve tracts were seen to be disrupted and no tracts were seen distal to the foramen (*arrow*). However, by placing the secondary region of interest on the distal side (*B*), though the nerve tracts were traced on the distal side, a deficit is seen in the foramen (*arrow*). In contrast, on the intact side of the left L5 root, there was no difference whether the ROI was proximal or distal.

Fig 4. Tractograms of 8 patients by placing the ROI on the proximal side of the foramen. In all patients, tracts show disruption of nerve fibers in the foramen (*arrows*).

Statistical Analysis

Statistical analyses were performed with StatView version 5.0 software (SAS Institute, Cary, North Carolina). A post hoc test was used to compare FA between healthy volunteers and patients with lumbar foraminal stenosis at L3–S1 nerve roots. Comparisons of nerve root FA values at the stenotic level between the entrapped side and intact side in the same subject also were conducted.

Bland-Altman plots of comparisons were used to determine inter- and intraobserver differences. Values of $P < .05$ were considered significant.

Results

Healthy Subjects

In all healthy volunteers, tractograms clearly showed all L3–S1 nerve roots and spinal nerve roots that symmetrically coursed obliquely downward (Fig 2). Mean ± SD L4–S1 FA values of nerves were 0.171 ± 0.035 for L3, 0.186 ± 0.026 for L4, 0.206 ± 0.029 for L5, and 0.201 ± 0.035 for S1. Mean FA values of the right and left side of the proximal nerve roots were 0.183 ± 0.028 and 0.184 ± 0.032, and for the right and left side of the distal spinal nerves were 0.198 ± 0.034 and 0.200 ± 0.038. Differences were not found between the right and left side nerves at the same lumbar segment (Table 1).

Subjects with Foraminal Stenosis

In patients, tractograms frequently showed abnormalities such as nerve tract disruption, narrowing, and indentation in their course through the foramen. Fiber tract reconstruction was performed by placing ROIs both proximal and distal to the foraminal zone at axial DTI maps. However, different tractograms were generated depending on whether the ROI placement was proximal or distal to the foramen only when foraminal stenosis existed. Figure 3 shows a sample tractogram by ROI placement on bilateral L5 roots at the stenotic level. ROIs were placed both proximally and distally to the foraminal zone at nonstenotic levels on L3, L4, and S1 roots.

On the entrapped side of the right L5 root, by placing the ROI on the proximal side (Fig 3*A*), nerve tracts were seen to be disrupted and no tracts were found distal to the foramen. However, by placing the secondary ROI on the distal side (Fig 3*B*), though the nerve tracts were traced on the distal side, a deficit is seen in the foramen. In contrast, on the intact side of the left L5 root, there was no difference whether the ROI was proximal or distal.

Figures 4 and 5 show tractograms of 7 patients. By placing the ROI on the proximal side of the foramen, in all patients, tracts reveal disruption of nerve fibers in the foramen (Fig 4). By placing the secondary ROI on the distal side

Fig 5. Tractograms of 8 patients by placing secondary ROI on the distal side of the foramen. Nerve traces show abnormalities (*white arrows*) such as tract disruption (case 1), nerve narrowing (cases 2–6), and indentation (cases 7 and 8) in their course through the foramen.

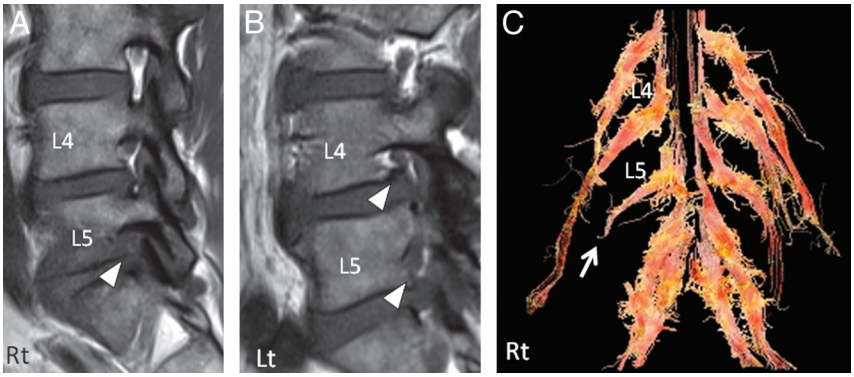

Fig 6. Sagittal T1-weighted MR images (*A*; right side, *B*; left side) and a diffusion tensor image (*C*) of a 62-year-old man with right L5–S1 foraminal stenosis (referenced as patient 4 in Table 3). Although asymptomatic foraminal stenosis on the left L4 and left L5 foramina (*arrowheads* in *B*) were found by MR imaging, abnormalities such as disruption of nerve fibers were only accurately detected at the symptomatic root by DTI (*arrow* in *C*).

Table 2: Incidence of detected foraminal narrowing in patients on MR imaging and DTI

	L4	L5	Total
MR imaging			
Asymptomatic foramina ($n = 24$)	5/16	6/8	11/24
Symptomatic foramina ($n = 8$)	0/0	8/8	8/8
False-positive rate (%)			45.80
DTI	L4	L5	Total
Asymptomatic foramina ($n = 24$)	0/16	0/8	0/24
Symptomatic foramina ($n = 8$)	0/0	8/8	8/8
False-positive rate (%)			0.00

of the foramen, nerve traces show abnormalities such as tract disruption (Fig 5, case 1), nerve narrowing (Fig 5, cases 2–6), and indentation (Fig 5, cases 7 and 8) in their course through the foramen.

Figure 6 shows sagittal MR images (T1-weighted) and a DTI from a patient (case 4; right L5 foraminal stenosis). Although asymptomatic foraminal stenosis on the left L4 and left L5 foramina were found by MR imaging, abnormalities such as disruption of nerve fibers were only accurately detected on symptomatic root by DTI. Table 2 shows the distribution of foraminal narrowing in patients on MR imaging and DTI. No abnormalities were seen in 32 foramens of healthy volunteers. Of 24 asymptomatic foramens in the patients, 11 instances (45.8%) of narrowing were detected by MR imaging. In contrast, no abnormalities (0.0%) of asymptomatic roots were detected by DTI.

The mean FA of proximal nerve roots on the side of entrapment was 0.128 ± 0.036, which is significantly lower than the 0.213 ± 0.042 on the intact side, and the mean FA of the distal spinal nerve roots on the side of entrapment was 0.131 ± 0.014, significantly lower than the 0.242 ± 0.032 seen on the intact side ($P < .001$; Fig 7 and Table 3). Differences were not found in FA between healthy volunteers and patients with lumbar foraminal stenosis at L3–S1 nerve roots. In this study, no significant observer variations or interobserver variance were found in the comparisons of FA values (Fig 8). The average leg pain VAS score in the 8 patients was 76.3, and there were no correlations between the FA and clinical parameters such as the VAS.

Discussion

Lumbar foraminal stenosis is a condition in which a nerve root or spinal nerve is entrapped in a narrowed lumbar foramen in degenerative lumbar spinal disorders.[1-6] The incidence of nerve root entrapment has been reported to be between 8 and 11% in degenerative lumbar disease.[22,23] A higher incidence of foraminal stenosis is found in the lower lumbar segments.[24,25] Jenis and An[4] reported that the most common roots involved are the L5 root (75%), followed by the L4 root (15%), the L3 root (5%), and the L2 root (4%), which is consistent with our findings. In its clinical presentation, severe leg pain at rest and

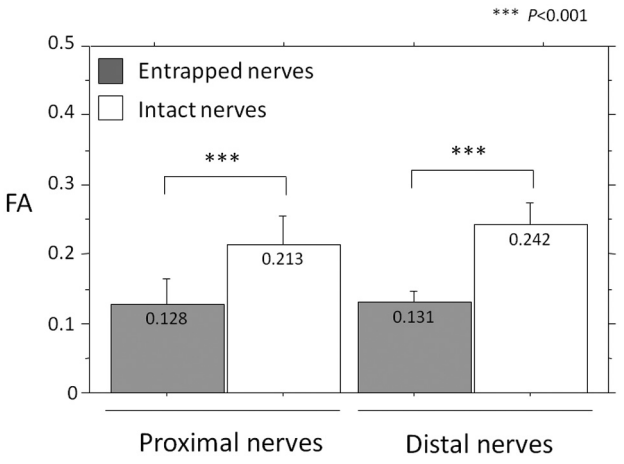

Fig 7. Mean FA values at the proximal nerve root and distal spinal nerve in patients with foraminal stenosis. The mean FA of proximal nerve roots on the side of entrapment was 0.155 ± 0.049 and is significantly lower than the 0.208 ± 0.036 on the intact side. The mean FA of distal spinal nerve roots on the side of entrapment was 0.131 ± 0.016 and significantly lower than the 0.240 ± 0.035 seen on the intact side ($P < .001$).

limited lumbar extension to the painful side (Kemp sign) were observed at high frequency.[23] Although imaging studies including radiography, CT, and MR imaging[26-29] provide an effective means for evaluating foraminal stenosis, these conventional imaging techniques do not detect foraminal stenosis with any certainty because false-positive findings may be frequently observed. Evaluation of clinical findings and selective nerve root infiltration and block are necessary to make a correct diagnosis.[30] This condition unfortunately results in failed back surgery syndrome because it is difficult to make a correct diagnosis, for which advanced neuroimaging techniques are required.

Although peripheral nerves cannot be selectively visualized by conventional MR imaging by using T1- and T2-weighted imaging, Yamashita et al[31] have demonstrated the feasibility of whole-body MR neurography with the use of DWI that can depict tissues with an impeded diffusion, such as tumors, brain, spinal cord, and peripheral nerves. MR neurography by using DWI can clearly show lumbar nerve roots, and the mean ADC in nerve root entrapment with foraminal stenosis is higher than in intact nerve roots in approximately a 10-minute scan time by using MR imaging at 1.5 T.[20] The ADC map is limited because the tissue contrast between nerves and surrounding tissues is poor.[15] In this study, we have shown that DTI can clearly show tractograms of lumbar nerve roots and determine FA values of the nerve roots in patients and healthy volunteers in approximately a 5-minute scan time by using MR imaging at 3T.

Olmarker et al[32] reported that slow onset of compression caused edema and demyelination in spinal nerve roots of pig cauda equina. Morphologic and histologic studies of patients with severe spinal stenosis confirm pathologic changes such as demyelination and axon loss in redundant roots.[33]

Regarding studies of diffusion MR imaging focused on the affected nerve, MacDonald et al[18] used a mouse brain injury model and showed that relative anisotropy and axial diffusivity were reduced by 6 hours to 4 days after trauma, corresponding to axonal injury; from 1 to 4 weeks after trauma, relative anisotropy remained decreased, whereas radial diffusivity increased, corresponding to demyelination, edema, and persistent axonal injury. Beaulieu et al[11,12] reported that wallerian degeneration after peripheral nerve injury reduces the anisotropy of water diffusion. Reports of several studies indicated that the FA values of peripheral nerves were strongly correlated with axonal degeneration and regeneration in rat and mouse sciatic nerves.[16,17] The findings indicated that the FA values were strongly correlated with axonal attenuation, which supports the hypothesis that axonal membranes play a major role in anisotropic water diffusion in neural fibers.

Previous studies of decreasing FA values in central nerve lesions and peripheral nerve compression have been reported.[15-18] To date, there are no studies assessing FA values of lumbar nerve roots by using DTI. In this present study, the mean FA values in entrapped nerve roots were lower than they were in intact nerve roots, indicating that diffusion in the tissue had become more isotropic because of edema, in which fluid is trapped in the tissue, creating an isotropic environment and a reduction in FA. In patients with foraminal stenosis, by placing the region of interest both proximal and distal to the foraminal zone, nerve fiber tracts could not be seen in the foramen because of the reduction of FA value.

For clinical use, tractography can provide anatomic information and accurate localization of nerve compression in the foramen, which can be helpful in surgical planning. Another advantage of DTI is that nerve fiber tracts can be directly visualized without making the maximum intensity projections necessary in DWI.

We acknowledge that our study has several limitations. The first is that a small number of subjects were investigated. Further studies are needed to investigate whether our findings

Table 3: Patient summary

No.	Age (yr)	Sex	Symptomatic Root	Disease Duration (mo)	VAS (Leg Pain)	DTI Findings	FA			
							Proximal		Distal	
							Entrapped	Intact	Entrapped	Intact
1	75	M	L5 (Right)	15	60	Tract disruption	0.0698	0.162	0.117	0.195
2	64	F	L5 (Left)	18	90	Tract disruption	0.086	0.185	0.148	0.278
3	66	M	L5 (Right)	8	70	Tract disruption	0.112	0.271	0.130	0.252
4	62	M	L5 (Right)	14	90	Tract disruption	0.165	0.238	0.124	0.223
5	47	M	L5 (Right)	24	80	Tract disruption	0.135	0.174	0.106	0.238
6	44	M	L5 (Left)	7	60	Tract disruption	0.128	0.200	0.138	0.242
7	64	F	L5 (Right)	24	100	Tract disruption	0.16	0.271	0.141	0.292
8	68	F	L5 (Right)	12	60	Tract disruption	0.166	0.203	0.143	0.214
Mean	61			15.2	76.3		0.128	0.213	0.131	0.242

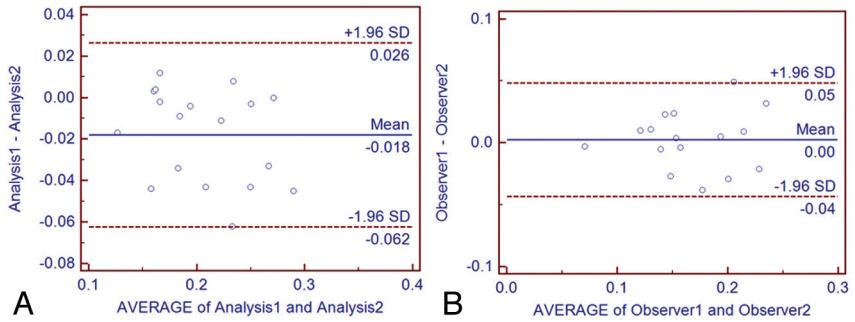

Fig 8. Bland-Altman plots of comparisons of FA values. Most observed differences are within mean ± 1.96 SD. Horizontal dashed lines indicate mean difference (middle line) and limits of agreement, defined as mean difference plus (top line) and minus (bottom line) 1.96 × SD of differences. *A,* Relationship between differences in the first analysis and second analysis (y-axis) and means of the first analysis and second analysis (x-axis). *B,* Relationship between differences in observer 1 and observer 2 (y-axis) and means of observer 1 and observer 2 (x-axis).

remain valid in a larger population. Second, we could not repeat the DTI after surgery because of spinal instrumentation artifacts such as those from pedicle screw systems. Third, when multiple axonal fibers and different fibers cross within the same voxel, diffusion anisotropy may become isotropic and directional information is lost as a result of the partial volume effect. Fourth, that tracts might be apparently missing in tractograms of patients with foraminal stenosis does not necessarily indicate loss of nerve fibers or paralysis but that there is some isotropic change and FA reduction. Moreover, the number of tracts visualized by DTI did not present the actual volume of nerve fiber trajectories. Finally, further studies are needed by using a stronger magnetic field, multiple acquisitions for each encoding gradient direction, and a longer examination time to significantly improve image quality, for example, by increasing the MR imaging signal intensity–to-noise ratio.

Conclusions

This preliminary study demonstrates that DTI can be used to visualize abnormalities such as nerve disruption, narrowing, and indentation in their course through the foramen and to quantitatively evaluate lumbar nerve entrapment in patients with foraminal stenosis. We believe that DTI has the potential to be used as a tool for the diagnosis of lumbar nerve entrapment.

References

1. Putti V. **New conceptions in the pathogenesis of sciatic pain.** *Lancet* 1927;2:53–60
2. Bose K, Balasubramaniam P. **Nerve root canals of the lumbar spine.** *Spine* 1984;9:16–18
3. Nowicki BH, Haughton VM, Schmidt TA, et al. **Occult lumbar lateral spinal stenosis in neural foramina subjected to physiologic loading.** *AJNR Am J Neuroradiol* 1996;17:1605–14
4. Jenis LG, An HS. **Spine update. Lumbar foraminal stenosis.** *Spine* 2000;25:389–94
5. Lee C, Rauschning W, Glenn W. **Lateral lumbar spinal canal stenosis: classification, pathologic anatomy, surgical decompression.** *Spine* 1988;13:313–20
6. Crock H. **Normal, pathologic anatomy of the lumbar spinal nerve root canals.** *J Bone Joint Surg Br* 1981;63B:487–90
7. Burton R, Kirkaldy-Willis W, Yong-Hing K, et al. **Causes of failure of surgery on the lumbar spine.** *Clin Orthop* 1981;157:191–97
8. MacNab I. **Negative disc exploration: an analysis of the causes of nerve root involvement in sixty-eight patients.** *J Bone Joint Surg Am* 1971;53:891–903
9. Aota Y, Niwa T, Yoshikawa K, et al. **Magnetic resonance imaging and magnetic resonance myelography in the presurgical diagnosis of lumbar foraminal stenosis.** *Spine* 2007;32:896–03
10. Basser PJ, Jones DK. **Diffusion tensor MRI: theory, experimental design and data analysis—a technical review.** *NMR Biomed* 2002;15:456–67
11. Beaulieu C, Allen PS. **Determinants of anisotropic water diffusion in nerves.** *Magn Reson Med* 1994;31:394–400
12. Beaulieu C, Does MD, Snyder RE, et al. **Changes in water diffusion due to wallerian degeneration in peripheral nerve.** *Magn Reson Med* 1996;36:627–31
13. Basser PJ, Pierpaoli C. **Microstructural and physiological features of tissues elucidated by quantitative-diffusion-tensor MRI.** *J Magn Reson B* 1996;111:209–19
14. Minematsu K, Fisher M, Li L, et al. **Diffusion-weighted magnetic resonance imaging: rapid and quantitative detection of focal brain ischemia.** *Neurology* 1992;42:235–40
15. Khalil C, Hancart C, Le Thuc V, et al. **Diffusion tensor imaging and tractography of the median nerve in carpal tunnel syndrome: preliminary results.** *Eur Radiol* 2008;18:2283–91
16. Lehmann HC, Zhang J, Mori S, et al. **Diffusion tensor imaging to assess axonal regeneration in peripheral nerves.** *Exp Neurol* 2010;223:238–44
17. Takagi T, Nakamura M, Yamada M, et al. **Visualization of peripheral nerve degeneration and regeneration: monitoring with diffusion tensor tractography.** *Neuroimage* 2009;44:884–92
18. MacDonald CL, Dikranian K, Bayly P, et al. **Diffusion tensor imaging reliably detects experimental traumatic axonal injury and indicates approximate time of injury.** *J Neurosci* 2007;27:11869–76
19. Fujiyoshi K, Yamada M, Nakamura M, et al. **In vivo tracing of neural tracts in the intact and injured spinal cord of marmosets by diffusion tensor tractography.** *J Neurosci* 2007;27:11991–98
20. Eguchi Y, Ohtori S, Yamashita M, et al. **Clinical applications of diffusion magnetic resonance imaging of the lumbar foraminal nerve root entrapment.** *Eur Spine J* 2010;19:1874–82
21. Masutani Y, Aoki S, Abe O, et al. **MR diffusion tensor imaging: recent advance and new techniques for diffusion tensor visualization.** *Eur J Radiol* 2003;46:53–66
22. Kunogi J, Hasue M. **Diagnosis and operative treatment of intraforaminal and extraforaminal nerve root decompression.** *Spine* 1991;16:1312–20
23. Porter R, Hibbert C, Evans C. **The natural history of root entrapment syndrome.** *Spine* 1984;9:418–21
24. Cohen M, Wall E, Brown R, et al. **Cauda equina anatomy: II. Extrathecal nerve roots and dorsal root ganglia.** *Spine* 1990;15:1248–51
25. Hasegawa T, Mikawa Y, Watanabe R, et al. **Morphometric analysis of the lumbosacral nerve roots and dorsal root ganglia by magnetic resonance imaging.** *Spine* 1996;21:1005–09
26. Hasegawa T, An H, Haughton V, et al. **Lumbar foraminal stenosis: critical heights of the intervertebral discs and foramina.** *J Bone Joint Surg* 1995;77:32–38
27. Kirkaldy-Willis W, Wedge J, Yong-Hing K, et al. **Lumbar spinal nerve lateral entrapment.** *Clin Orthop* 1982;169:171–78
28. Vanderlinden RG. **Subarticular entrapment of the dorsal root ganglion as a cause of sciatic pain.** *Spine* 1984;9:19–22
29. Krudy AG. **MR myelography using heavily T2-weighted fast spin-echo pulse sequences with fat presaturation.** *AJR Am J Roentgenol* 1992;159:1315–20
30. Herron L. **Selective nerve root block in patient selection for lumbar surgery: surgical results.** *J Spinal Disord* 1989;2:75–79
31. Yamashita T, Kwee TC, Takahara T. **Whole-body magnetic resonance neurography.** *N Engl J Med* 2009;361:538–39
32. Olmarker K, Rydevik B, Holm S. **Edema formation in spinal nerve roots induced by experimental, graded compression: an experimental study on the pig cauda equina with special reference to differences in effects between rapid and slow onset of compression.** *Spine* 1989;14:569–73
33. Suzuki K, Takatsu T, Inoue H, et al. **Redundant nerve roots of the cauda equina caused by lumbar spinal canal stenosis.** *Spine* 1992;17:1337–42